Electronic Supporting Information (ESI):

A novel active mitochondrial selective fluorescent probe for NIR fluorescence imaging and targeted photodynamic therapy of gastric cancer

Jie Ding, [‡ab], Xing Kang, [‡b], Min Feng, [‡b], Jiangkun Tan, [‡c], Qingzhao Feng [a], Xingzhou Wang [b], Jiafeng Wang [b], Jiang Liu [d], Zan Li *[c], Wenxian Guan *[b], and Tong Qiao *[ae]

[a] *Department of General Surgery, Nanjing Drum Tower Hospital Clinical College of Nanjing Medical University, Nanjing, 210008, China.*

[b] *Department of General Surgery, Nanjing Drum Tower Hospital, The Affiliated Hospital of Nanjing University Medical School, Nanjing, 210008, China.*

[c] *Key Laboratory of Life-Organic Analysis of Shandong Province, School of Chemistry and Chemical Engineering, Qufu Normal University, Qufu, 273165, China.*

[d] *Department of General Surgery, Jiangsu Province Hospital of Chinese Medicine, Nanjing, 210004, China.*

[e] *Department of Vascular Surgery, Nanjing Drum Tower Hospital, The Affiliated Hospital of Nanjing University Medical School, Nanjing, 210008, China.*

**Correspondence authors: qiaotongmail@nju.edu.cn, lizan@qfnu.edu.cn, 15850502391@163.com*

‡ *These authors contributed equally to this work.*

Table of Contents

Materials and Instrumentation

The general chemicals used in this study were purchased from Aladdin Biochemical Technology Co., LTD, and all solvents in this study were analytical grade. Singlet Oxygen detection probe 1,3-Diphenylisobenzofuran (DPBF) was purchased from Aladdin Biochemical Technology Co., Ltd. TUNEL apoptosis kit was purchased from Roche Ltd. cRGD((fk)-3-Mal）was obtained from China Peptides Co., Ltd. Mitochondria Tracker, Lysosome Tracker, Cytomembrane Tracker, Endoplasmic Reticulum Tracker, Hoechst 33342 and 2, 7-dichlorofluorescein diacetate (DCFH-DA) Detection Kit were purchased from Beyotime Biotechnology Co., Ltd. Cytomembrane Tracker were purchased from Jiangsu KeyGEN Biotechnology Co., Ltd. Anti-GAPDH, anti-integrin α_5, anti-integrin β_1 and secondary antibody goat anti-rabbit IgG were purchased from Abcam (USA).

NMR spectra were detected by a Bruker AVANCE III HD-500 spectrometer. Electrospray ionization Mass spectrometric (ESI-MS) data were obtained with LC-MS Agilent G6460A spectrometer. Absorption were detected with a UV-3600 plus visible spectrophotometer (Shimadzu Co., Ltd.). Fluorescence emission spectra, fluorescence quantum yields (QY) and fluorescence lifetimes were determined on a FLS1000-stm spectrophotometer (Edinburgh Instruments). NIR fluorescence imaging were performed on LSM880NLO two-photon fluorescence microscope (Carl Zeiss, Germany) in cell experiments. Small animals' fluorescence imaging was carried out by IVIS LUMINA III XR living imaging system (PerkinElmer, USA). Using Mettler Toledo S210 pH meter detected pH value.

Synthesis of Cy_{683}, Cy_{620}, Cy_{1395}

Cy_{683} was prepared according to the method previously reported.[1] IR-813 (604.30 mg, 0.80 mmol) and 1-butylamine (73.1 mg, 1.0 mmol) were added to 20 mL of DMF and the mixture was reflux for 12 hours. After the reaction, the mixture was extracted three times with dichloromethane and brine. The crude products were purified by silica gel column chromatography by elution with dichloromethane/methanol at 200:1 to 20:1. Red solids (215.40 mg, 32.50 %) were obtained as **Cy_{620}**. The product was characterized by ESI-MS (**Fig. S1**), calcd. for $C_{44}H_{50}N_3^+$ $[M]^+$: 620.3999; found: 620.3999. ^1H (500 MHz, $CDCl_3$) δ 8.08 (2 H, s), 7.83 (5 H, dd, J 16.5, 8.4), 7.52 (3 H, s), 7.34 (2 H, t, J 7.4), 7.17 (2 H, s), 5.50 (2 H, s), 3.92 (1 H, s), 3.40 (6 H, s), 2.54 (4 H, s), 2.02 (12 H, d, J 13.1), 1.84 (2 H, dt, J 12.8, 6.5), 1.70

(2 H, s), 1.44–1.37 (2 H, m),1.25 (2 H, s), 0.95 (3 H, t, J 7.1) (**Fig. S2**). ^{13}C (126 MHz, CDCl3) δ 167.76, 141.05, 130.94, 130.46, 129.80, 129.69, 128.84, 128.72, 127.12, 123.27, 121.96, 109.33, 93.03, 65.48, 53.48, 33.02, 28.27, 25.72, 21.65, 20.17, 19.16, 13.76 (**Fig. S3**).

IR-813 (1510.66 mg, 2.0 mmol), 1,2-ethanedithiol (377.0 mg, 4.0 mmol) and 1 mL of triethylamine were added to 30 mL of DMF and the mixture was reflux under argon for 2 hours. The mixture was then extracted three times with dichloromethane and brine. The solvent is then vaporized under reduced pressure. The crude products were purified by silica gel column chromatography by elution with 200:1 to 15:1 dichloromethane/methanol. Yellow-green solid (364.0mg, 28.40 %) was obtained. The product was characterized by ESI-MS (**Fig. S4**), calcd for $C_{42}H_{45}N_2S_2^+$ $[M]^+$: 641.3019; found: 641.3038. **^{1}HNMR** (500MHz,$CDCl_3$) δ 8.00 (s,1H), 7.79 (s,2H), 7.48 (s,1H), 7.28 (s,2H), 7.15 (s,1H), 6.93 (s,1H), 5.33 (s,1H), 5.26 (s,1H),4.56-4.22 (m,4H), 3.94 (s,6H), 3.72 (s,4H), 3.35 (s,2H), 3.28 (s,4H), 2.49 (s,2H), 2.26 (s,7H), 1.90 (s,7H), 1.81 (s,9H), 1.45 (s,14H), 1.29 (s,8H), 1.16-0.74 (m,44H), 0.63 (s,9H) (**Fig. S5**). **^{13}C NMR**(126 MHz,$CDCl_3$) δ 155.55, 154.05, 140.78, 139.40, 130.67, 129.99, 129.90, 128.58, 127.48, 123.63, 122.69, 121.74, 117.69, 109.15, 75.05, 59.45, 58.85, 56.60, 56.11, 53.45, 50.03, 49.82, 49.04, 42.27, 39.69, 39.50, 38.79, 36.95, 36.53, 36.43, 36.16, 35.77, 31.86, 29.97, 28.39, 28.32, 28.22, 28.20, 28.00, 24.29, 23.82, 22.82, 22.56, 21.04, 19.39, 18.71, 11.87 (**Fig. S6**).

Cy_{641} (307.68 mg, 0.48 mmol) and cRGD(fk)-3-mal (301.6 mg, 0.4 mmol) were dissolved in 50 mL of water/acetonitrile (1:1 v/v) mixed solution, and the solution was reacted at 4℃ for 24 h under nitrogen protection. After the reaction, the crude product was lyophilized to remove the solvent, and the green crude product was obtained. Little sample was taken and analyzed on HPLC to determine the target peak time. Preparation was performend by C18 reversed-phase chromatography system: Wavelength: 220 nm, The Flow Rate: 15 ml/min, Vol: 20mL, Column Temp: 25 °C: Buffer 1: An aqueous solution containing 0.1 % trifluoroacetic (TFA) aqueous solution, Buffer 2: Acetonitrile solution containing 0.1 % trifluoroacetic acid; Collect the target peak solution and lyophilize the solution to obtain the green product (107.1 mg, 19.2 %) as Cy_{1395}. The product was characterized by ESI-MS (**Fig. S7**), calcd. for $C_{76}H_{91}N_{12}O_{10}S_2^+$ $[M]^+$: 1395.6417; found:1395.6417. **^{1}H NMR** (500 MHz, DMSO) δ 8.83 (d, J = 14.2 Hz, 2H), 8.37 (s, 1H), 8.29 (d, J = 8.5 Hz, 2H), 8.13 (s, 1H), 8.11 (s, 1H), 8.10 (s, 1H), 8.09 (s, 1H), 8.07

(s, 1H), 8.06 (s, 1H), 8.01 (d, *J* = 7.2 Hz, 1H), 7.90 (t, *J* = 5.2 Hz, 1H), 7.77 (d, *J* = 8.9 Hz, 2H), 7.71 (dd, *J* = 11.5, 6.8 Hz, 2H), 7.66 (t, *J* = 7.7 Hz, 2H), 7.51 (t, *J* = 7.5 Hz, 2H), 7.22 (t, *J* = 7.5 Hz, 2H), 7.14 (t, *J* = 7.6 Hz, 3H), 6.34 (d, *J* = 14.3 Hz, 2H), 4.65 (dd, *J* = 14.4, 8.4 Hz, 1H), 4.43 (dd, *J* = 14.1, 7.2 Hz, 2H), 4.18 (dd, *J* = 14.3, 7.8 Hz, 2H), 4.06 (dd, *J* = 15.1, 7.7 Hz, 2H), 4.01 – 3.98 (m, 1H), 3.97 – 3.92 (m, 1H), 3.80 (s, 6H), 3.57 – 3.52 (m, 2H), 3.25 (dd, *J* = 14.9, 3.8 Hz, 1H), 3.16 – 3.13 (m, 3H), 3.11 – 3.05 (m, 3H), 2.95 – 2.87 (m, 4H), 2.80 (dd, *J* = 13.3, 5.6 Hz, 1H), 2.71 (d, *J* = 7.5 Hz, 4H), 2.44 (dd, *J* = 18.3, 3.8 Hz, 1H), 2.37 (dd, *J* = 16.2, 5.7 Hz, 1H), 2.29 – 2.25 (m, 2H), 1.99 (d, *J* = 2.4 Hz, 12H), 1.90 – 1.85 (m, 2H), 1.74 – 1.71 (m, 1H), 1.54 – 1.45 (m, 2H), 1.41 – 1.34 (m, 3H), 1.26 – 1.19 (m, 3H), 1.02 – 0.95 (m, 2H) (**Fig. S8**). **^{13}C NMR** (126 MHz, DMSO) δ 176.81, 175.12, 174.00, 172.57, 172.17, 171.58, 170.96, 170.40, 169.98, 169.40, 158.93, 158.66, 157.25, 153.35, 143.97, 141.03, 137.80, 133.58, 133.39, 131.86, 130.75, 130.41, 129.55, 128.55, 128.20, 127.96, 126.70, 125.26, 122.69, 118.21, 115.85, 112.09, 101.76, 54.98, 54.87, 52.24, 50.91, 49.32, 43.72, 40.74, 40.58, 38.74, 37.89, 36.79, 36.18, 35.56, 33.34, 32.16, 31.59, 31.41, 28.95, 28.75, 27.32, 26.30, 25.65, 23.30, 21.08 (**Fig. S9**).

Fluorescence spectrum of Cy_{641} and Cy_{1395}

The fluorescence spectrum of Cy_{641} and Cy_{1395} in ethanol (10 μM) were detected by fluorescence spectrometer.

Fluorescence lifetime and quantum yields of Cy_{1395}

The fluorescence lifetime and quantum yields (QY) of Cy_{1395} were measured by a fluorimeter (FLS-1000) with excitation (λex) =700 nm.

Singlet Oxygen Detection

The singlet oxygen generated by **Cy_{683}**, **Cy_{620}**, **Cy_{1395}** and methylene blue (MB) was measured using DPBF. In DMSO, the absorbance of DPBF was adjusted to about 1.0 at 415 nm, the absorbance of targeted molecule was adjusted to about 0.3. Then, 808 nm laser (For Cy683 and Cy1395), and 660 nm (For Cy620 and MB) were used to irradiate samples for different times, and absorption spectra were measured immediately. Φ Δ was calculated by the following equation:

$$\Phi\Delta\mathrm{sam} = \Phi\Delta\mathrm{std}\left(\frac{S_{sam}}{S_{std}}\right)\left(\frac{F_{std}}{F_{sam}}\right)$$

Where ΦΔ represents singlet oxygen yield, "sam" and "std" represent "fluorescent molecules" and "MB" respectively. "*S*" is the slope of linear fitting that the x-axis represents the radiation time and the y-axis represents the UV absorption value of DPBF at 415 nm after corresponding irradiation time. *F* is the absorption correction factor of test compound and reference compound, $F = 1\text{-}10^{-OD}$ (O.D. represents the absorbance of solution at 808 nm).

Preparation and Characterization of Cy_{1395}-NPs

In brief, 10 mg of Cy_{1395} was dissolved in 0.72 mL DMSO, ultrasonic ensure uniform dissolved, then 0.72 mL of ultrapure water was slowly added. Continuous ultrasound for 0.5 h and obtained Cy_{1395} nanoparticles (Cy_{1395}-NPs) suspension liquid, the solution was stored at 4 °C. The morphology of the Cy_{1395}-NPs was evaluated through TEM (JEOL, Japan) at 120 kV. The particle size and size distribution of the Cy_{1395}-NPs were detected at 25˚C by Nano-particle analyzer (Malvern Instruments, UK). The stability of the Cy_{1395}-NPs suspension liquid was evaluated by particle size analysis at different time points (Repeat test 3 times for the sample).

Optical properties and biological stability of Cy_{1395}-NPs

The absorption and fluorescence spectrum of Cy_{1395}-NPs in different value pH solutions (pH=5, 6, 7, 7.4, 8, 9) and in fetal bovine serum (FBS) of different density (0 %, 5 %, 10 %, 20 %, 50 %, 100 %) were detected by UV and fluorescence spectrometer respectively. Absorption spectra of Cy_{1395}-NPs in 20 % FBS at different times (0, 6, 12, 24 and 48 h) were also detected. For fluorescence emission spectra, the excitation wavelength is 700 nm. The concentration of all tested samples was diluted to 10 μM.

Cell lines and culture conditions

The human gastric mucosal endothelial cell line GES1 and human gastric cancer cell lines AGS, MKN45 were obtained from Shanghai Institute of cell biology, Chinese Academy of Sciences. Dulbecco's modified eagle's medium (DMEM) contain 10 % fetal bovine serum (FBS), 100 U/ml penicillin and 100 μg/ml streptomycin (GIBCO, USA) were used for cell culture, at 37 °C in a humid environment containing 5 % of CO_2.

Mice and subcutaneous transplanted tumor models

Healthy male ICR mice (4-5 weeks old, 18-20 g) and male BALB/C nude mice (4-5 weeks old, 16–18 g) with severe combined immunodeficiency (SCID) were purchased from Jinan Peng Yue Experimental Animal Breeding Co., LTD. The feeding environment was SPF grade,

the pad materials were treated by irradiation sterilization, and the drinking water was pure water. In order to establish the tumor model of gastric cancer, the concentration of MKN45 cells were 5×10^6 in 50 μL normal saline, and the cells were injected subcutaneously into the armpit of the right leg of isoflurane anesthetized nude mice. The calculated tumor volume is (π / 6 × long × width^2).

Western blot analysis

The whole cell lysate was prepared as described in the reference.[2] The concentration of whole protein was detected through Bicinchoninic acid protein detection kit (Beyotime, China). The same amount (35 μg) of protein was extracted from cultured cells, run on 10 % SDS-PAGE, and then electrically transferred to polyvinylidene fluoride membrane (Millipore, USA). The membranes were sealed with 5 % skimmed milk powder for 3 h, then mixed with anti-GAPDH (1:1000), anti-integrin α_v (1:1000) and anti-integrin β_3 (1:1000) incubated at 4 °C overnight, next the secondary antibody goat anti-rabbit IgG coupled with horseradish peroxidase was incubated at 25 °C for 2 h. The membranes were observed by chemiluminescence (Beyotime, China) and exposed in a darkroom with Gel Imager System (Cytiva, Japan). Finally, the gray level analysis is carried out with quantity one software.

Cellular uptake of Cy_{1395}-NPs

The logarithmic growth GES1, MKN45 and AGS cells were seeded onto a six-well plates (Corning, 353046) with an inoculation density of 1.0×10^5 cells/well and allowed growing for 24 h. In order to obtain the ideal cultivation conditions, the MKN45 cells were incubated with Cy_{1395}-NPs (10 μM) at different time (1, 3, 6 h) or with varying concentration of Cy_{1395}-NPs (5, 10, 30 μM) for 3 h and with Hoechst 33342 for another 15 min at 37°C. Then the binding effect of Cy_{1395}-NPs were further evaluated, GES1, MKN45 and AGS cells were incubated with Cy_{1395}-NPs (10 μM) for 3 h and with Hoechst 33342 for another 15 min at 37 °C. The fluorescence images were acquired by two photon fluorescence microscope at the red channel 600–700 nm with an excitation at 543 nm, the blue channel 410–460 nm with an excitation at 405 nm. Finally, ZEN software was used to analyze the mean fluorescence intensity.

Colocalization studies

To study the intracellular location of Cy_{1395}-NPs, MKN45 cells were co-incubated with Cy_{1395}-NPs (10 μM) for 3 h, with 0.1 μg/mL Hoechst 33342, 100 nM Mitochondria Tracker

(Mito-Tracker Green), 50 nM Lysosome Tracker (Lyso-Tracker Green), 5 nM Cytomembrane Tracker (Cyto-Tracker Green), 0.5 nM Endoplasmic Reticulum Tracker (ER-Tracker Green) for another 20 min. The medium was then removed, washed with cold PBS for three times, and 3 mL of PBS was added into each well for fluorescence imaging. Under the excitation of 543 nm, the emission of Cy_{1395}-NPs was collected in the red channel of 620–700 nm. Under the excitation of 405 nm, honchest 33345 was collected the emission on the blue channel of 410–460 nm. Under the excitation of 500–540 nm, Mito-Tracker, Lyso-Tracker, Cyto-Tracker and ER-Tracker were collected the emission under the excitation of 488 nm on the green channel of 500–540 nm.

Cytotoxicity and Photo-Cytotoxicity

The cytotoxicity and Photo-Cytotoxicity were measured by 3-(4,5-Dimethylthiazol-2-yl)-2,5-diphenyltetrazolium bromide (MTT) assay. For cytotoxicity, 10000 cells per well, GES1 and MKN45 cells were inoculated into 96 well plates and cultured overnight. Remove medium, GES1 and MKN45 cells were incubated with fresh medium with different concentrations of Cy_{1395}-NPs (0, 1, 2, 5, 7.5, 10, 12.5, 15 and 20 μM), after 3 h, culture medium was changed and continued for 24 h at 37 ℃. The cytotoxicity of DMSO was evaluated by the same method. For photo-cytotoxicity, the MKN45 cells were inoculated on 96-well plates (10000cells/well) and incubated at 37 ºC for overnight. The medium was replaced with a fresh medium with different Cy_{1395}-NPs concentrations (0, 1, 2, 5, 7.5, 10, 12.5, 15 and 20 μM) or with Cy_{1395}-NPs (10 μM), replacing fresh medium, then, the cells were irradiated for 60 s or different times (0, 10, 20, 40, 60, 90, 120 and 150 s) with a laser (808 nm,1W/cm^2) and incubated at 37 °C for another 24 h. The viability of cell is calculated from the following formula：

$$\text{Cell viability (\%)} = \left(\frac{OD_{eg} - OD_{bc}}{OD_{nc} - OD_{bc}}\right) \times 100\ \%$$

Where “eg”, “nc” and “bc” represent the “experiment group”, “negative control” and “blank control”, respectively. (OD. is the absorbance of the solution at 490 nm).

Intracellular Singlet Oxygen Detection

DCFH-DA Detection Kit was used to detect the generation of singlet oxygen of Cy_{1395}-NPs in MKN45 cells. The cells were firstly incubated in the cell culture plate for 24 h, then they were divided into seven groups: 1) cells were incubated with medium for 3 h; 2) cells were

under laser irradiation (1W/cm^2, 3 min); 3) cells were incubated with reactive oxygen control reagent (Rosup) for 0.5 h; 4) cells were co-cultured with 10 μM of Cy_{1395}-NPs for 3 h; 5) cells were incubated with 10 μM of Cy_{1395}-NPs for 3 h and under laser irradiation (1W/cm^2, 3 min); 6) cells were incubated with 10 μM of Cy_{1395}-NPs and 15 mM NAC for 3 h and under laser irradiation (1W/cm^2, 3 min); 7) cells were incubated with 10 μM of Cy_{1395}-NPs for 3 h and under laser irradiation (1W/cm^2, 3 min) in ice bath. Then, green images were obtained through fluorescence microscope (λex = 488 nm, λem = 500–540nm for green channel) and fluorescence intensity were analyzed by ZEN software.

***In vivo* Biodistribution and Biosafety**

To study the biodistribution of Cy_{1395}-NPs *in vivo*, 15 healthy male ICR mice with similar body weight were injected with Cy_{1395}-NPs (2 mg/Kg) via tail vein, the mice were randomly divided into 5 groups (n=3). 1) Fluorescence imaging was performed with IVIS LUMINA III XR imaging system at 0 h, 0.5 h, 3 h, 16 h, 40 h and 64 h post injection; 2-5)The mice were sacrificed at 0.5 h, 3 h, 16 h and 40 h post-injection, respectively, major organs including heart, liver, spleen, lung and kidney were isolated for fluorescence imaging. The fluorescence intensity of each organ was calculated by imaging software.

For biosafety, nine male ICR healthy mice were divided into 3 groups randomly (n=3). 1). Control group. 2) Cy_{1395}-NPs (2 mg/Kg) was injected and the mice were euthanized at 10 days after injection. 3) Cy_{1395}-NPs was injected and the mice were euthanized at 24 days after injection). All mice were injected with Cy_{1395}-NPs every other day for 3 times and blood was collected for hematological and biochemical analysis, including white blood cells (WBC), red blood cells (RBC), platelets (PLT), alanine aminotransferase (ALT), aspartate aminotransferase (AST), blood urea nitrogen (BUN) and creatinine (Cr). In addition, six male ICR normal mice with similar body weight were divided into 2 groups randomly (n=3). 1) PBS was injected; 2) Cy_{1395}-NPs was injected. The injection method is the same as above. Body weight of the mice were monitored in the two groups. 24 days after treatment, the mice were sacrificed and major organs were isolated for pathological analysis, including heart, liver, spleen, lung and kidney. To observe the pathology changes, all organs were immersed in 4 % paraformaldehyde for 6 h and embedded in paraffin. Then H&E staining was used to observe the histopathological changes under light microscope (NINGBO SUNNY INSTRUMENTS,

China).

NIR fluorescence imaging in tumor models

To monitor the targeted efficacy of Cy_{1395}-NPs in *vivo*, we established transplantation tumor model and six nude mice with similar tumor volume (~100 mm^3) were selected for the experiment. Oxygen/air mixture of 2.5 % isoflurane was used to anesthetize and fluorescence imaging was performed with IVIS LUMINA III XR imaging system at collection time points of 0, 1, 2, 4, 16, 20, 24, 32, 40, 48, 56 and 72 h post injection, respectively, three of them were sacrificed 40 h post-injection and the major organs (heart, liver, spleen, lung, kidney) and tumors were taken out for in *vitro* fluorescence imaging. The imaging conditions were set as follows: λex = 720 nm, λem = 845 nm, automatic exposure time, F/stop = 8, field of vision = 10.2x10.2 cm^2. The mean fluorescence intensity of tumor sites in *vivo* and major organs and tumor tissue in *vitro* were calculated via imaging software.

Photodynamic therapy in tumor models

When the tumor volume reached about 100 mm^3 after inoculation of MKN45 cells, the nude mice were randomly divided into four groups (n=3) for different treatments: PBS alone; PBS plus 808 nm laser irradiation (PBS + Laser); Cy_{1395}-NPs alone (Cy_{1395}-NPs); Cy_{1395}-NPs plus 808 nm laser irradiation (Cy_{1395}-NPs + Laser). After 40 h post-injection, tumor region was irradiated with 808 nm laser at 0.5 W/cm^2 for 5 min. The tumor sizes (long and width) acquired with an electronic vernier caliper and body weights were weighed with electronic balance. After treatment of 21 days, all nude mice were sacrificed and the tumors were collected, tumor tissues were weighed and photographed. Finally, H&E staining and TUNEL detection were used for histopathological analysis.

Statistical analysis

Data are expressed as mean ± standard deviation. Student's t-test was used to analyze the statistical significance. $P < 0.05$ was statistically significant. SPSS 19.0 software was used for statistical analysis.

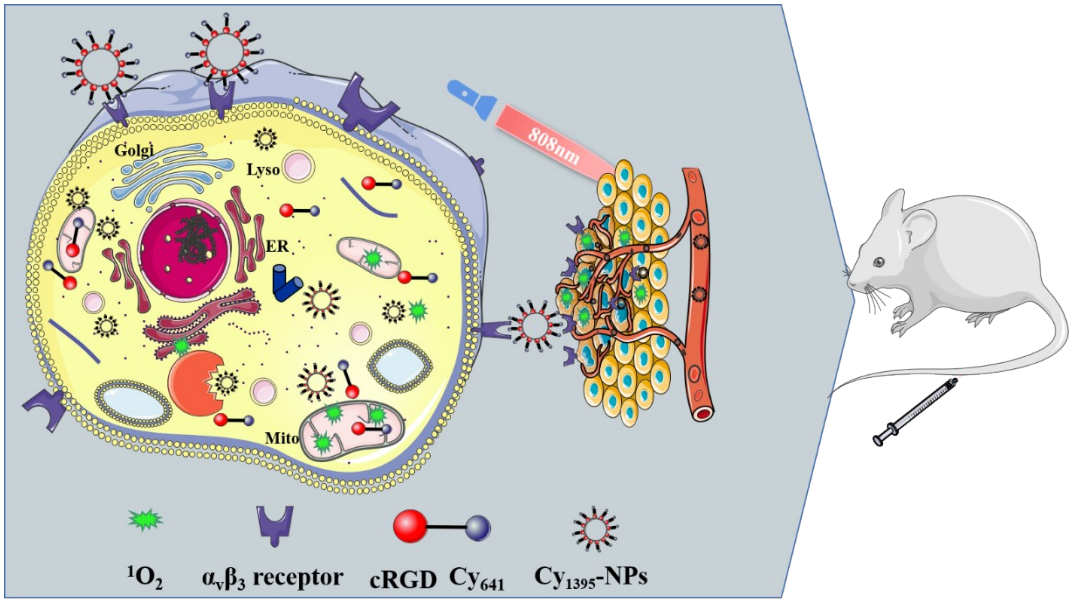

Scheme S1. Schematic illustration of the mechanism of Cy1395-NPs for fluorescence imaging and PDT of gastric cancer in vivo. After intravenous injection, Cy1395-NPs can selectively enter and accumulate in gastric cancer through active targeting mediated by integrin αvβ3, and selectively accumulate in the mitochondria. Realizing in NIR fluorescence imaging and PDT efficacy by the production of singlet oxygen with an 808 nm laser irradiation, ultimately inducing irreversible tumor inhibition.

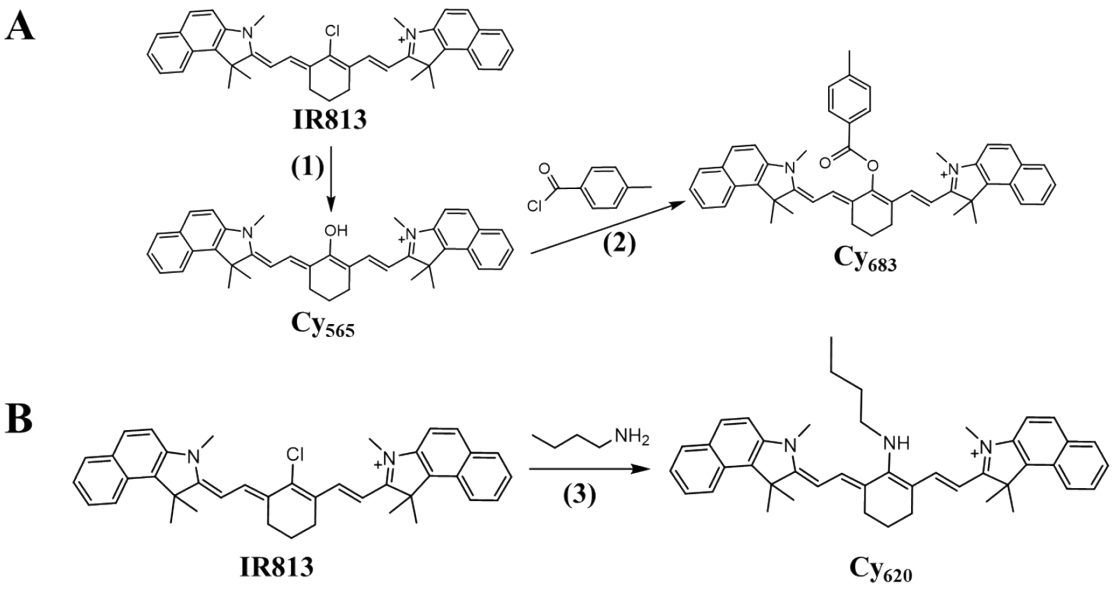

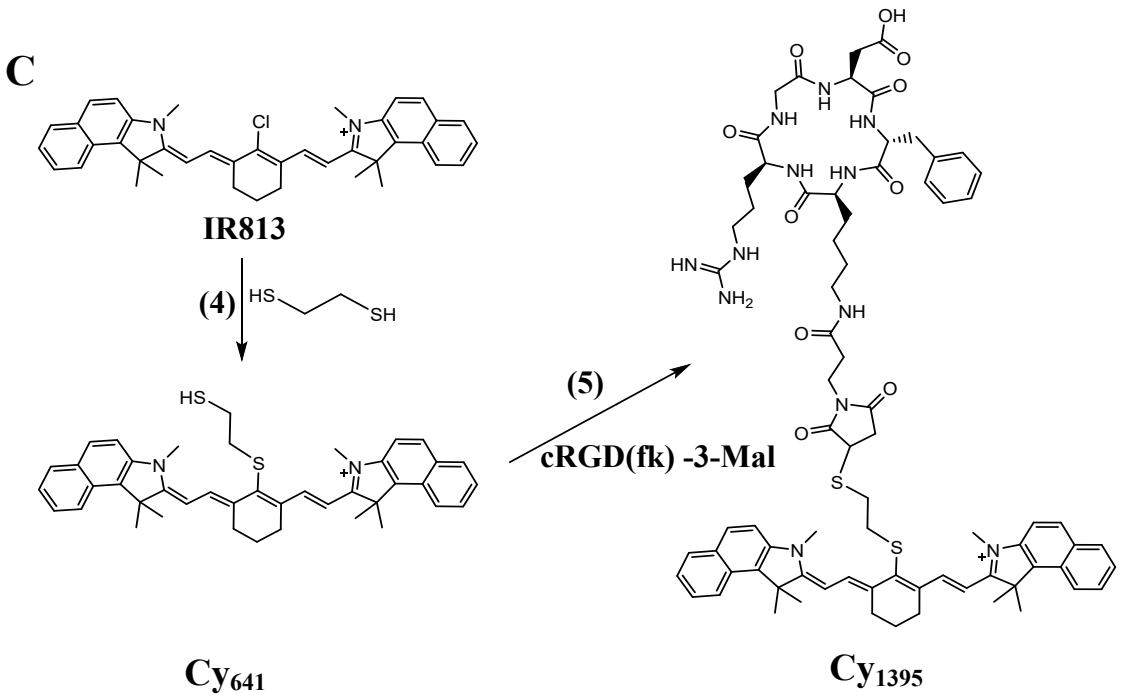

Scheme S2. Synthesis routes of Cy_{683} (A), Cy_{620} (B) and Cy_{1395} (C). **(1)** Sodium acetate, DMF, N_2, 70 °C, 10 h, **(2)** DCM, N_2, 25 °C, 12h/triethylamine, 25 °C, 30 min, **(3)** DMF, reflux,12 h, **(4)** triethylamine, DMF, reflux,2 h, **(5)** H_2O/ACN, N_2, 4 °C, 24 h.

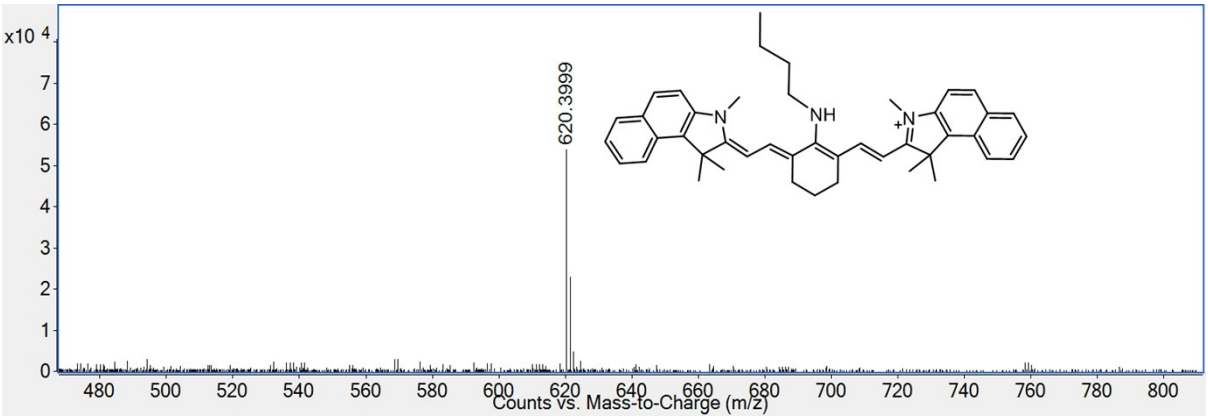

Figure S1. Electrospray ionization Mass spectrometric of Cy_{620}.

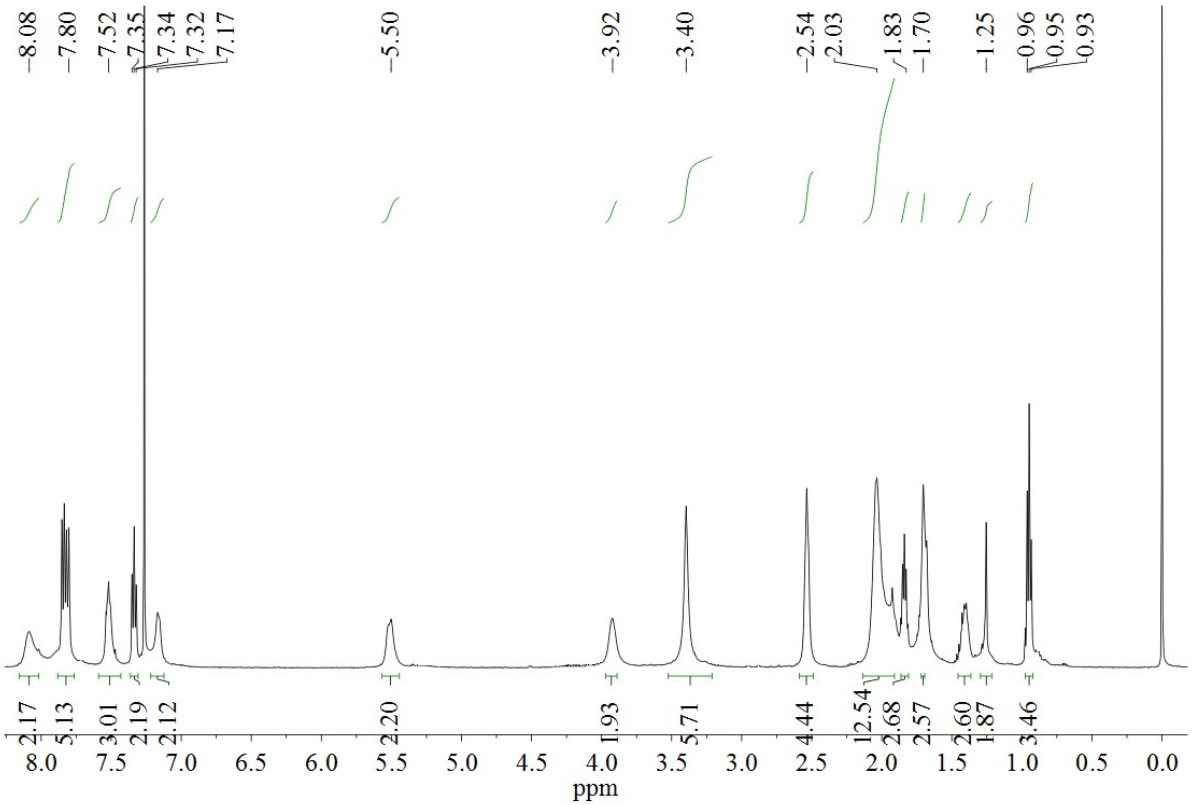

Figure S2. ^{1}H NMR spectrum of Cy_{620}.

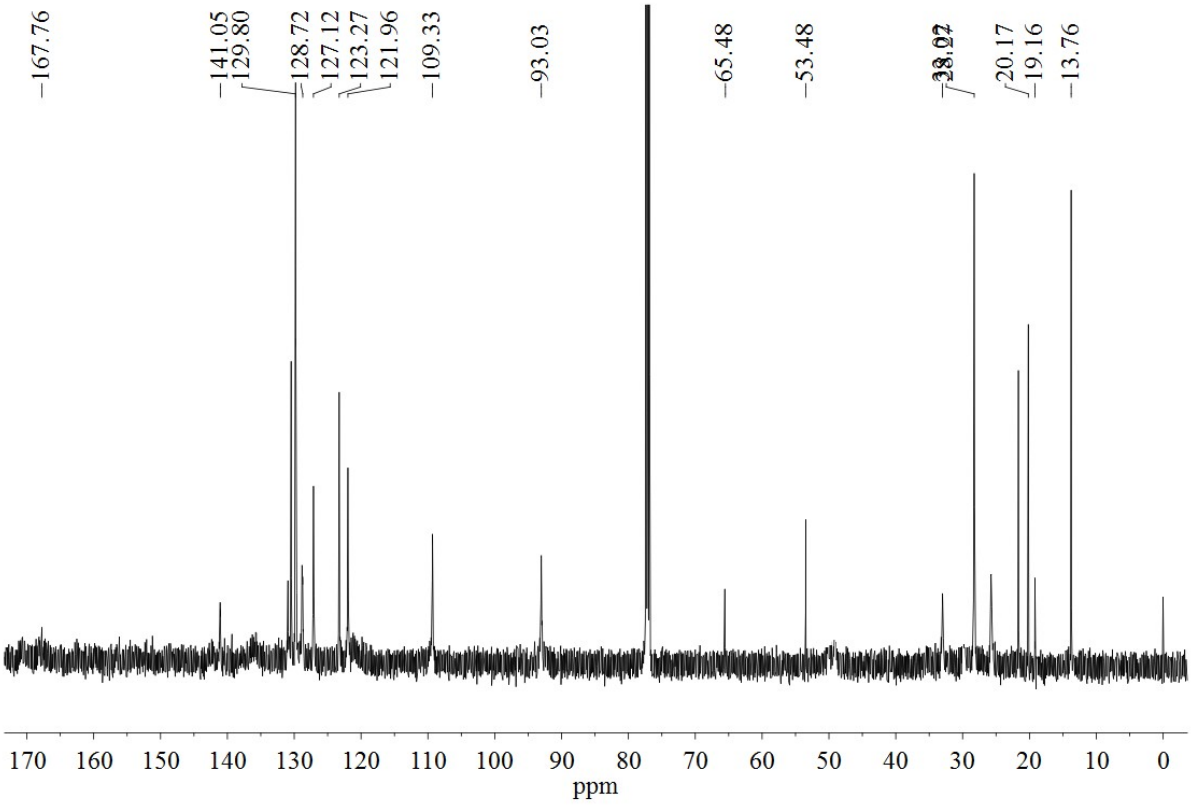

Figure S3. ^{13}C NMR spectrum of Cy_{620}.

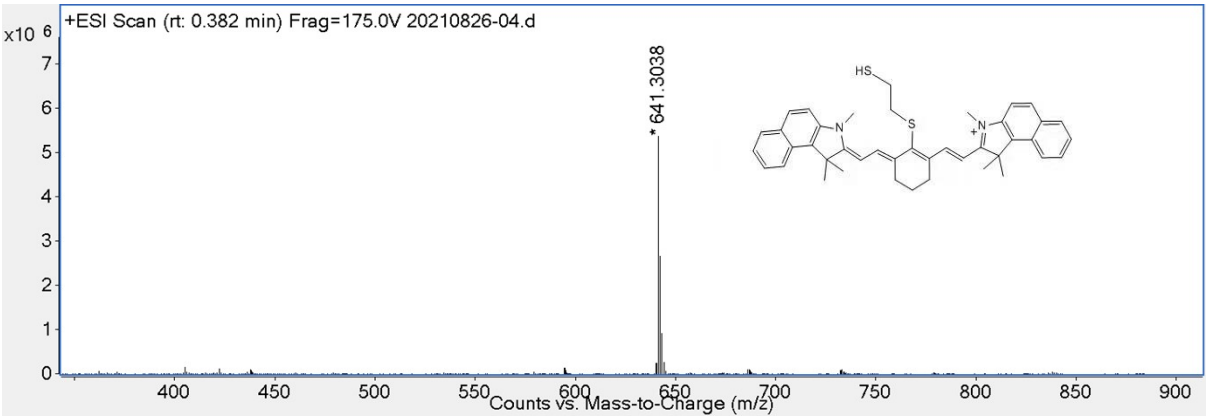

Figure S4. Electrospray ionization Mass spectrometric of Cy_{641}.

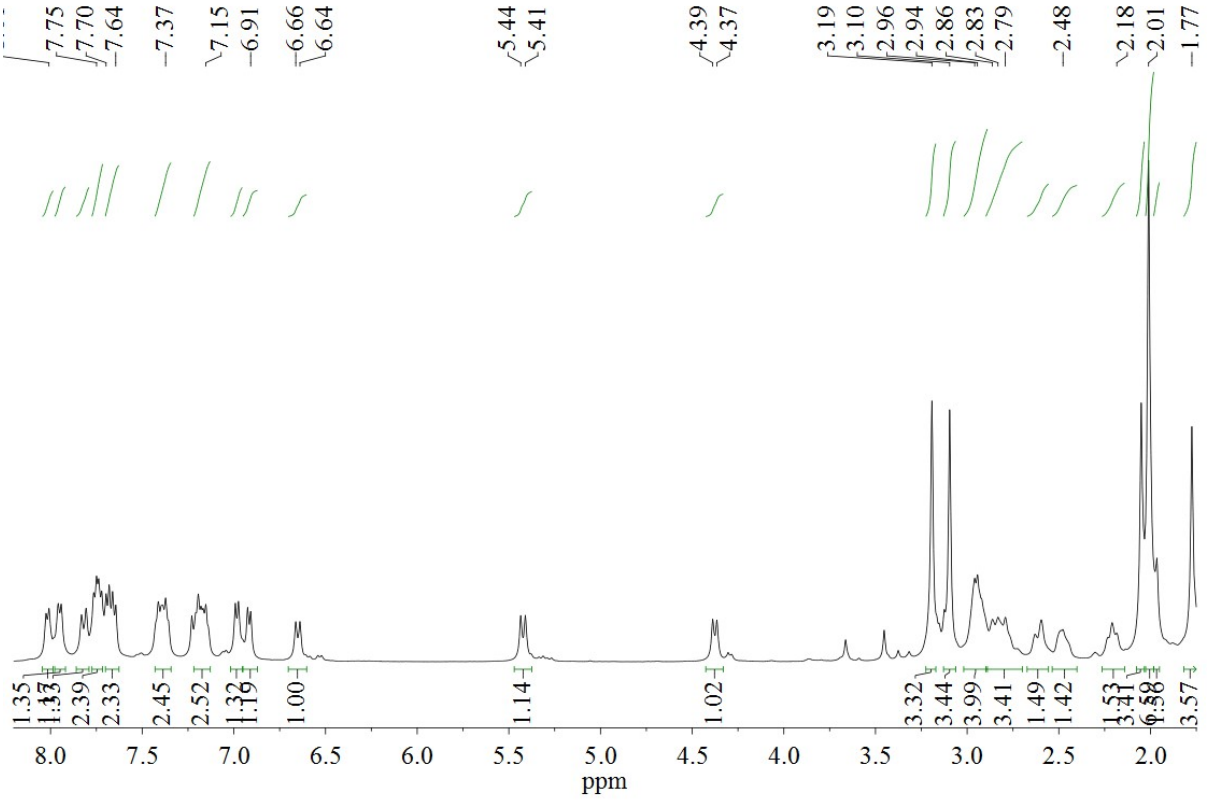

Figure S5. ^{1}H NMR spectrum of Cy_{641}.

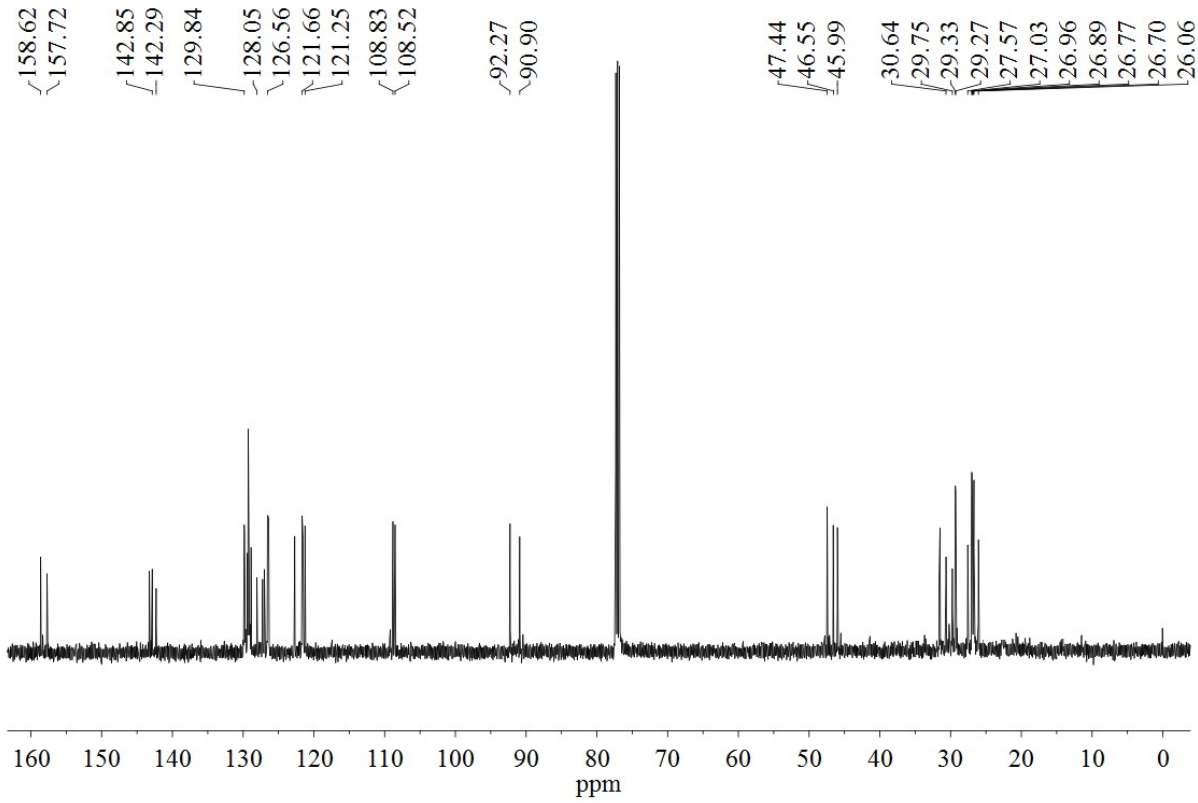

Figure S6. ^{13}C NMR spectrum of Cy_{641}.

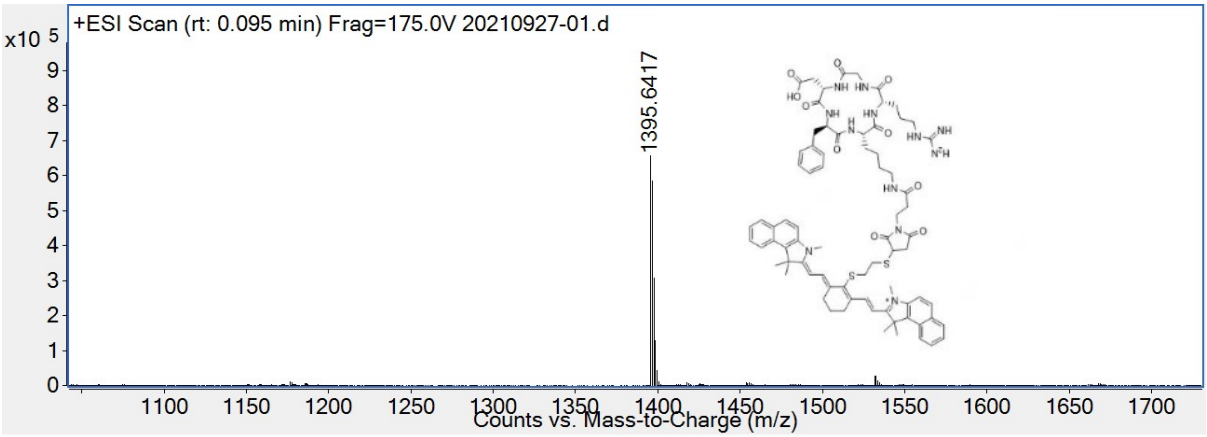

Figure S7. Electrospray ionization Mass spectrometric of Cy_{1395}.

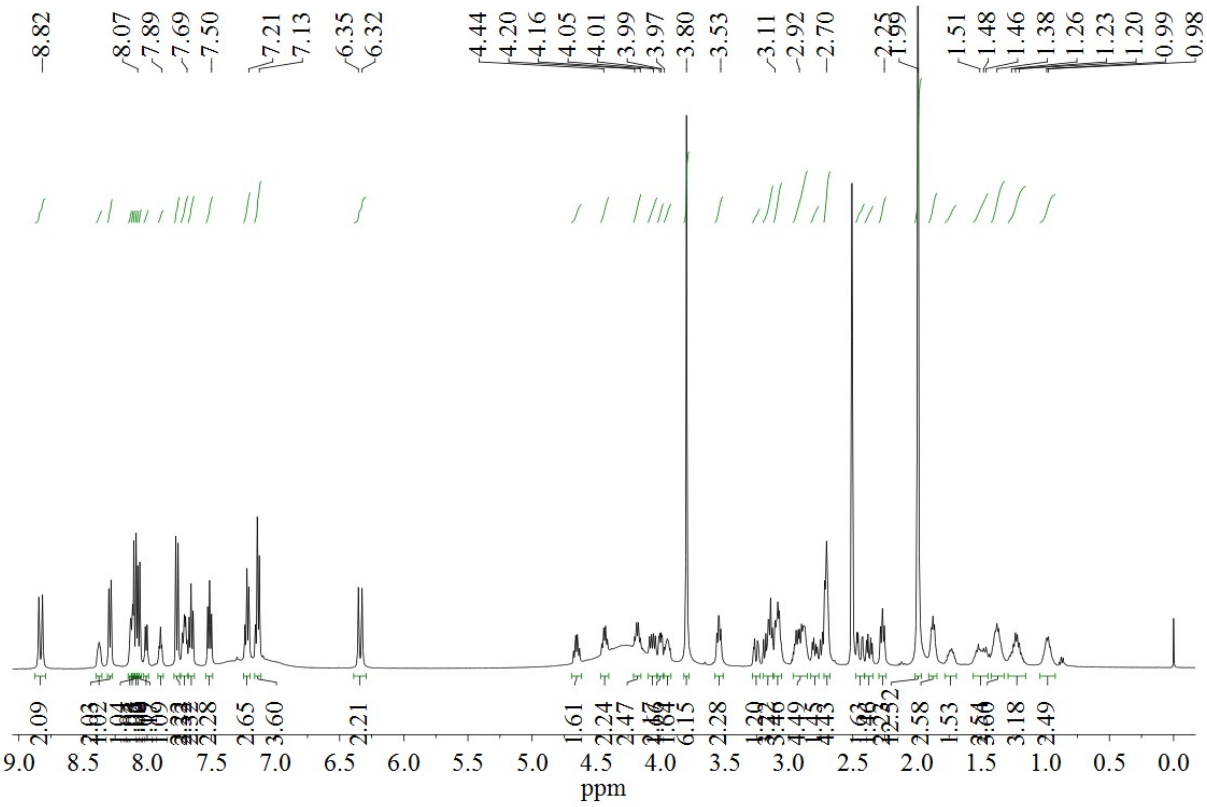

Figure S8. ^{1}H NMR spectrum of Cy_{1395}.

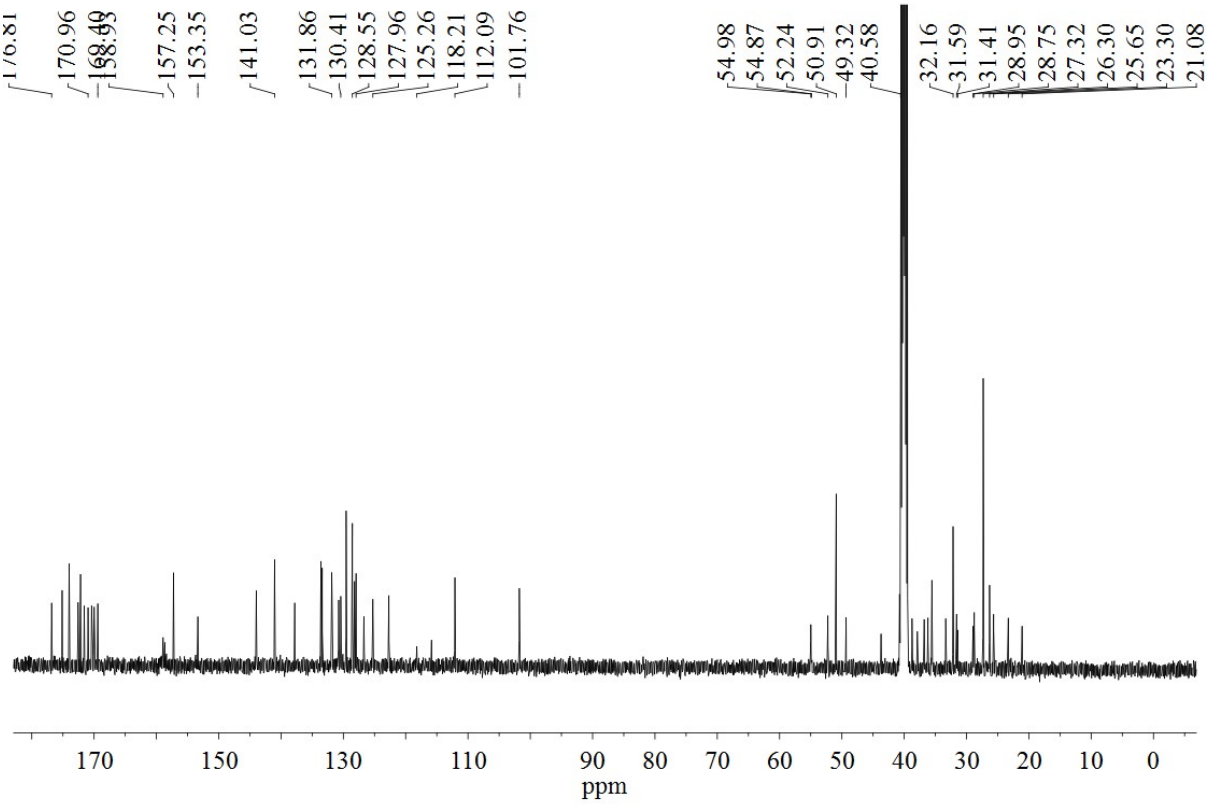

Figure S9. ^{13}C NMR spectrum of Cy_{1395}.

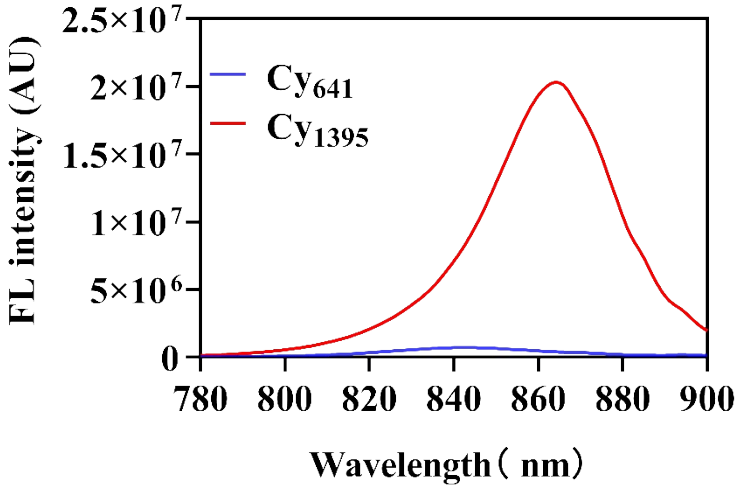

Figure S10. The fluorescence intensity of Cy_{641} and Cy_{1395} in ethanol (10 μM).

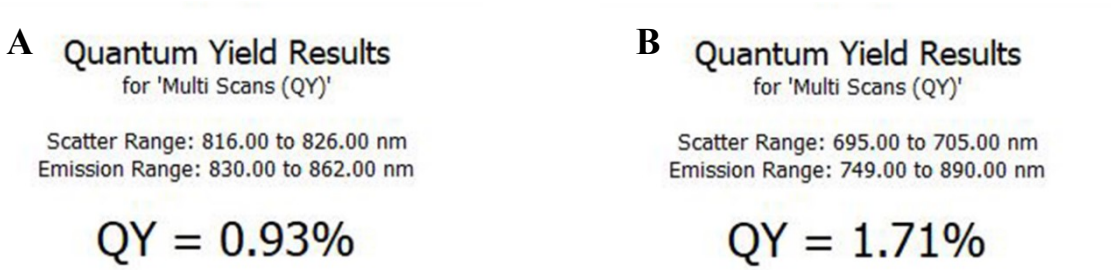

Figure S11. Fluorescence quantum yields of (A) Cy_{641} and (B) Cy_{1395} in MeOH.

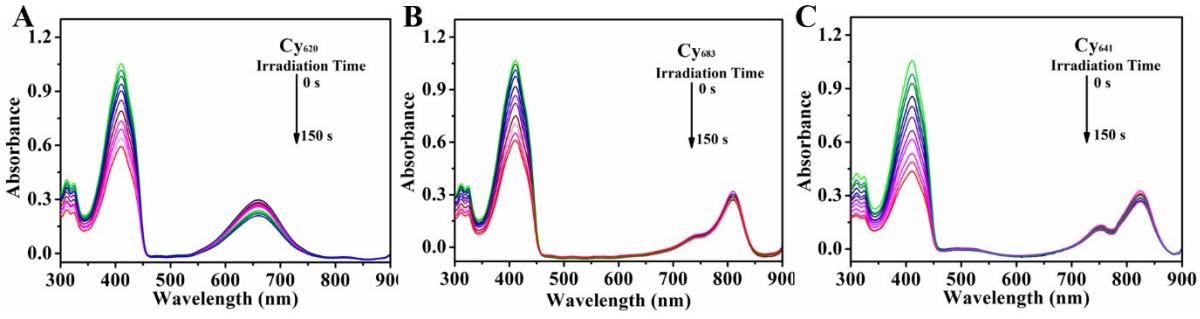

Figure S12. The absorbance changes of DPBF at 415 nm induced by (A) Cy_{620} under 660 nm

irradiation and (B) Cy_{683} and (C) Cy_{641} under 808 nm irradiation.

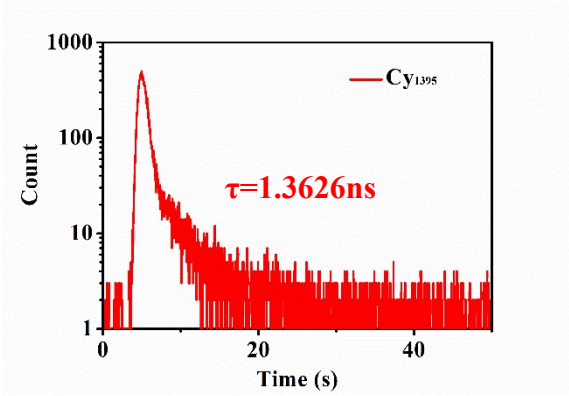

Figure S13. Fluorescence lifetime of Cy_{1395} in MeOH.

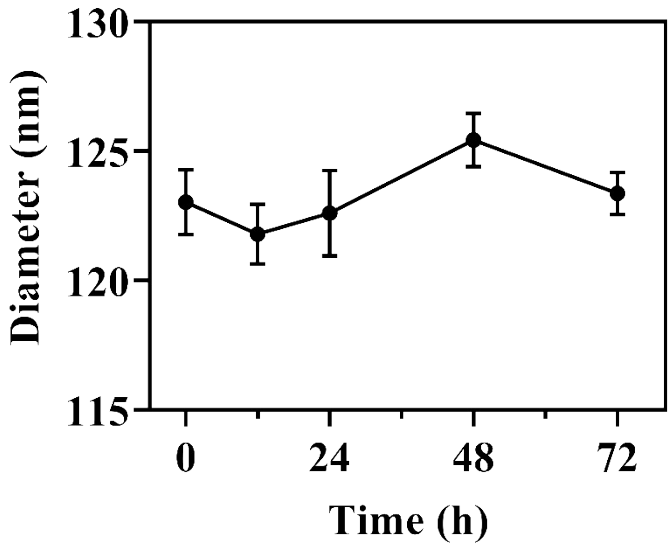

Figure S14. Particle size of Cy_{1395}-NPs at different times.

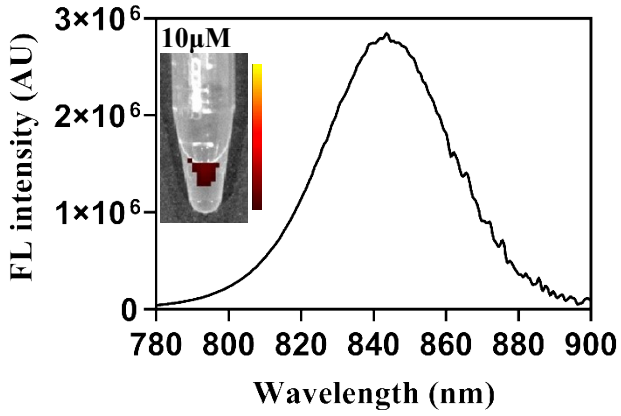

Figure S15. Fluorescence spectrum of Cy_{641} (10 μM), and fluorescence imaging of 10 μM

solution in methanol.

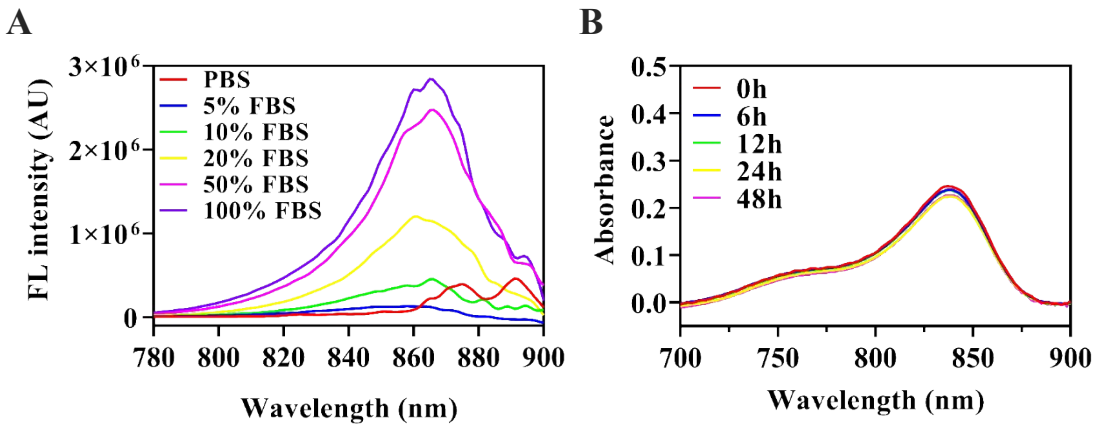

Figure S16. (A) Fluorescence spectrum of Cy_{1395}-NPs in FBS, (B) Absorption spectra of Cy_{1395}-NPs at different time in 20 % FBS.

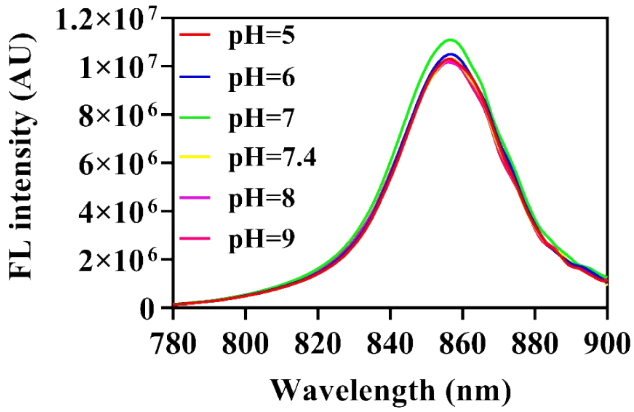

Figure S17. Fluorescence spectrum of Cy_{1395}-NPs at different pH solutions.

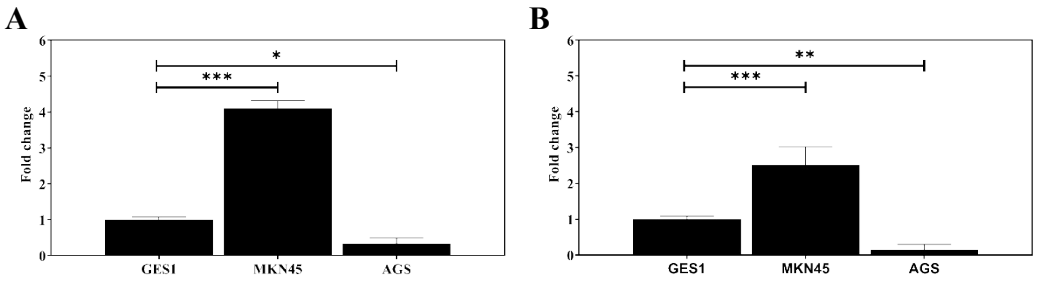

Figure S18. Gray level analysis of integrin α_V (A) and β_3 (B) subunit protein expression in human GES1, MKN45 and AGS cells (* P <0.05, ** P <0.01, *** P <0.001, compared with GES1 cells).

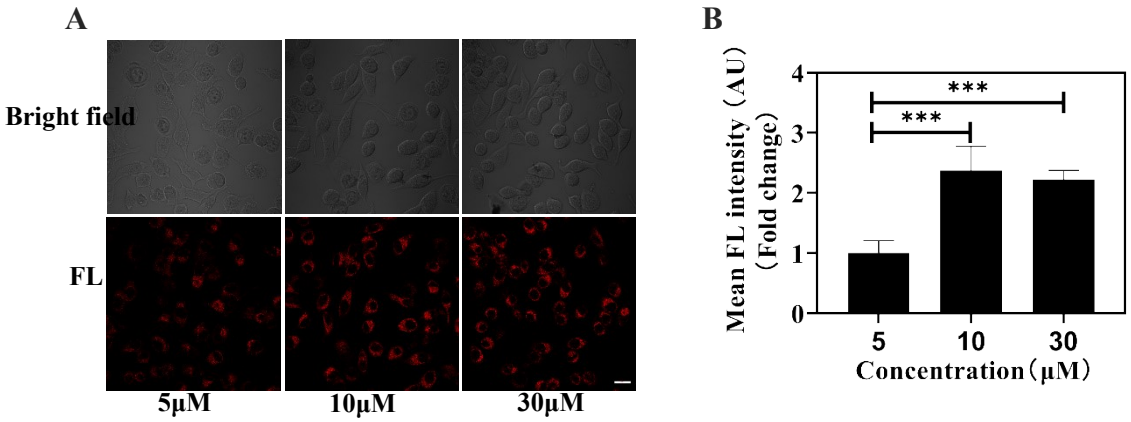

Figure S19. (A) Fluorescence images of MKN45 cells following incubation with different concentrations of Cy_{1395}-NPs (5 μM, 10 μM and 30 μM) for 3 h (λex = 543 nm, λem = 600-700 nm, scale bars = 20 μm), (B) Fold changes of mean fluorescence intensity of Cy_{1395}-NPs in 5 μM, 10 μM and 30 μM (*** P <0.001, compared with 5 μM). The fluorescence inside MKN45 cells reached the maximum after co-culture for 10 μM.

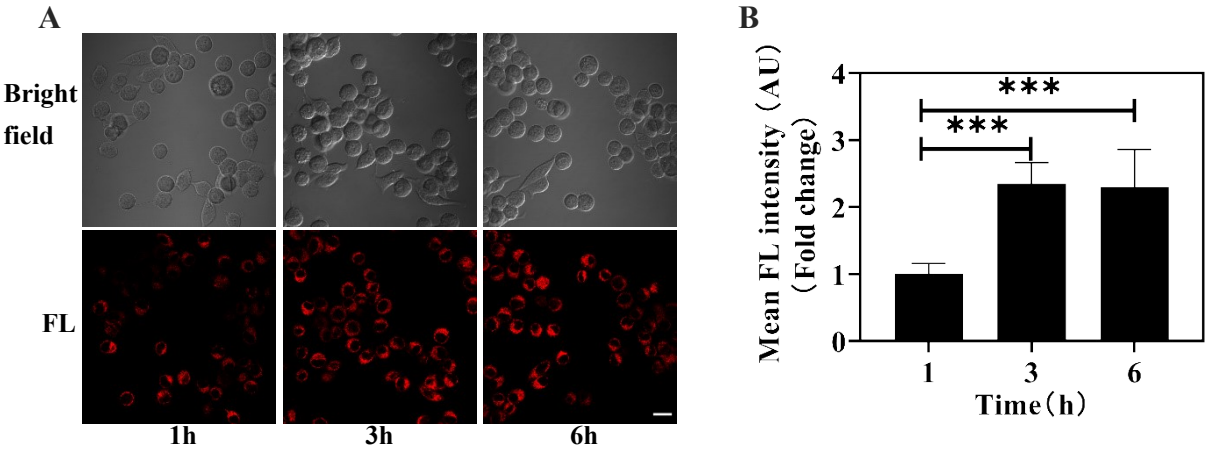

Figure S20. (A) Fluorescence images of MKN45 cells following incubation with Cy_{1395}-NPs

(10 μM) for different time (1 h, 3 h and 6 h) (λex = 543 nm, λem = 600-700 nm, scale bars = 20 μm), (B) Fold changes of mean fluorescence intensity of Cy_{1395}-NPs in 1 h, 3 h and 6 h (B) (*** P <0.001, compare to 1 h), The fluorescence inside MKN45 cells reached the maximum after co-culture for 3 h.

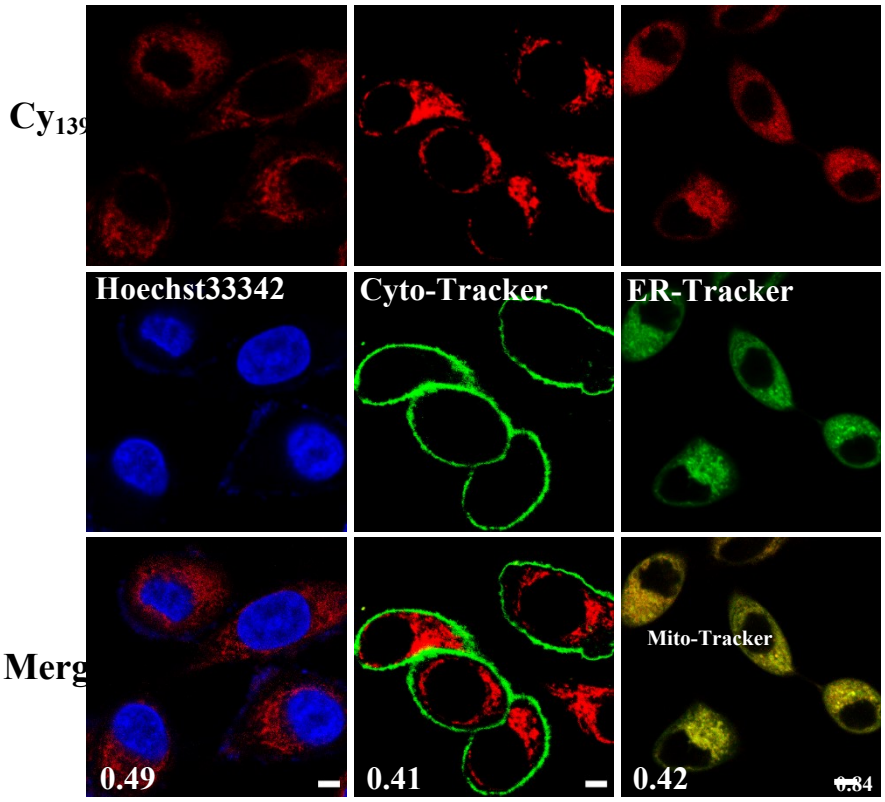

Figure S21. Co-localization fluorescence images of Cy_{1395}-NPs in MKN45 cells. MKN45 cells were incubated with Cy_{1395}-NPs (10 μM) for 3 h and with Hoechst33342, Cyto-Tracker and ER-Tracker for another 20 min. The blue channel represents Hoechst33342 (λex = 405 nm, λem = 410-460 nm); The red channel represents Cy_{1395}-NPs (λex = 543 nm, λem = 600-700 nm); Green channels represent Cyto-Tracker and ER-Tracker (λex = 488 nm, λem = 500-540 nm); scale bars=5 μm.

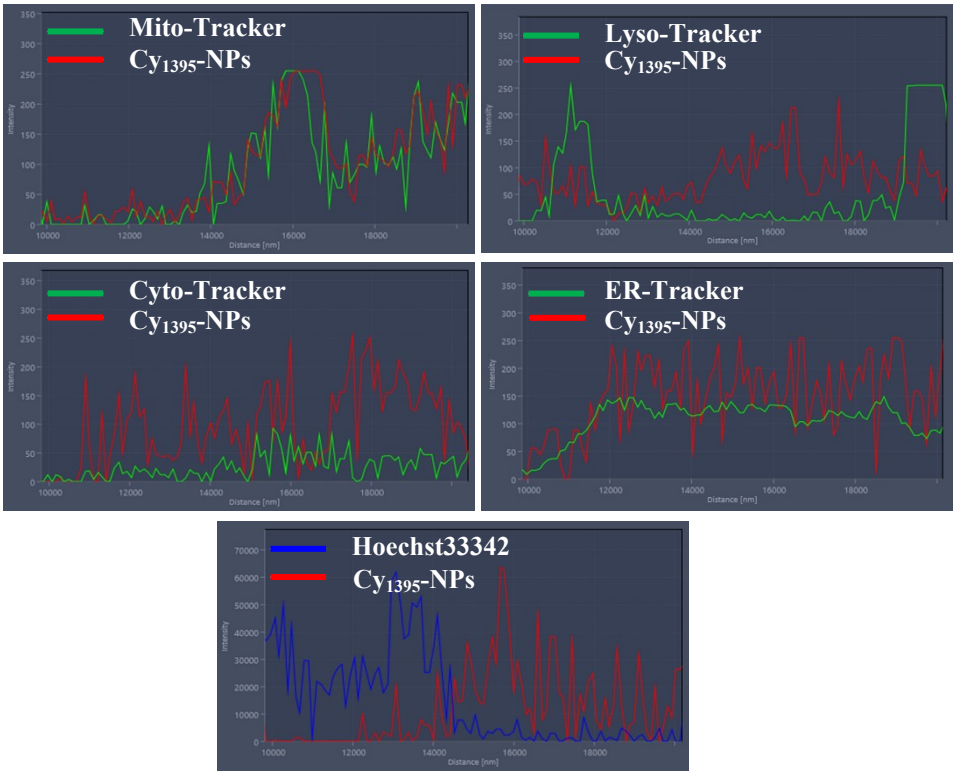

Figure S22. Colocalization analysis of released Cy_{1395}-NPs in MKN45 cells with Mito-Tracker, Lyso-Tracker, Cyto-Tracker, ER-Tracker and Hoechst33342.

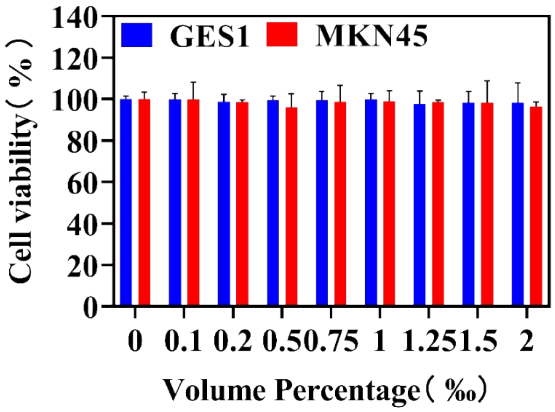

Figure S23. Cell viability of GES1 and MKN45 incubated with different volume ratio DMSO (0, 0.1, 0.2, 0.5, 0.75, 1, 1.25, 1.5, 2 ‰) for 3 h.

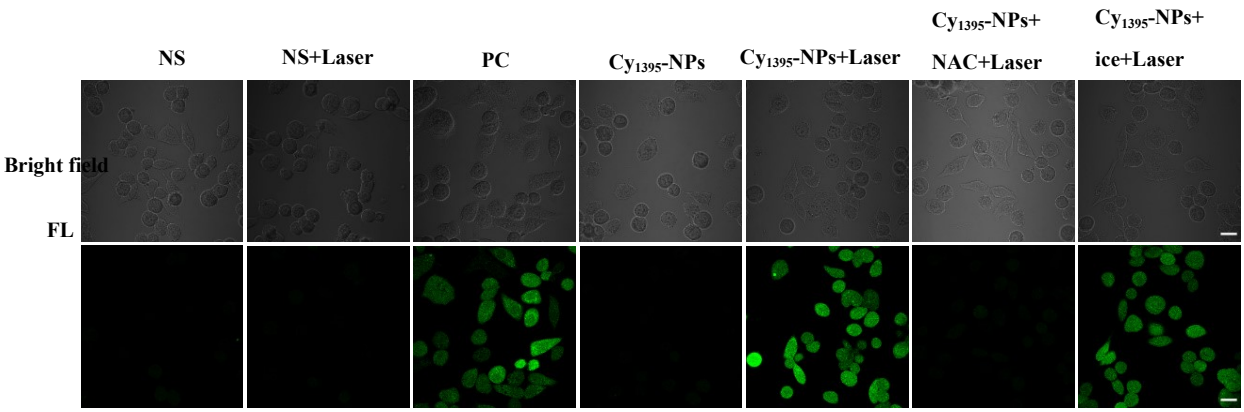

Figure S24. Fluorescence images of intracellular $^1O_2$ production by Cy_{1395}-NPs in MKN45 cells using the DCFH-DA assay. MKN45 cells were incubated with Cy_{1395}-NPs (10 μM) for 3 h and DCFH-DA for 30 min in different groups (NS: normal saline group; NS + laser group; PC: positive control group (Rousp); Cy_{1395}-NPs group; Cy_{1395}-NPs + laser group; Cy_{1395}-NPs + NAC+ laser group; Cy_{1395}-NPs + ice bath + laser group (1W/cm^2, 3 min, λex = 488 nm, λem = 500-540 nm, scale bars = 20 μm).

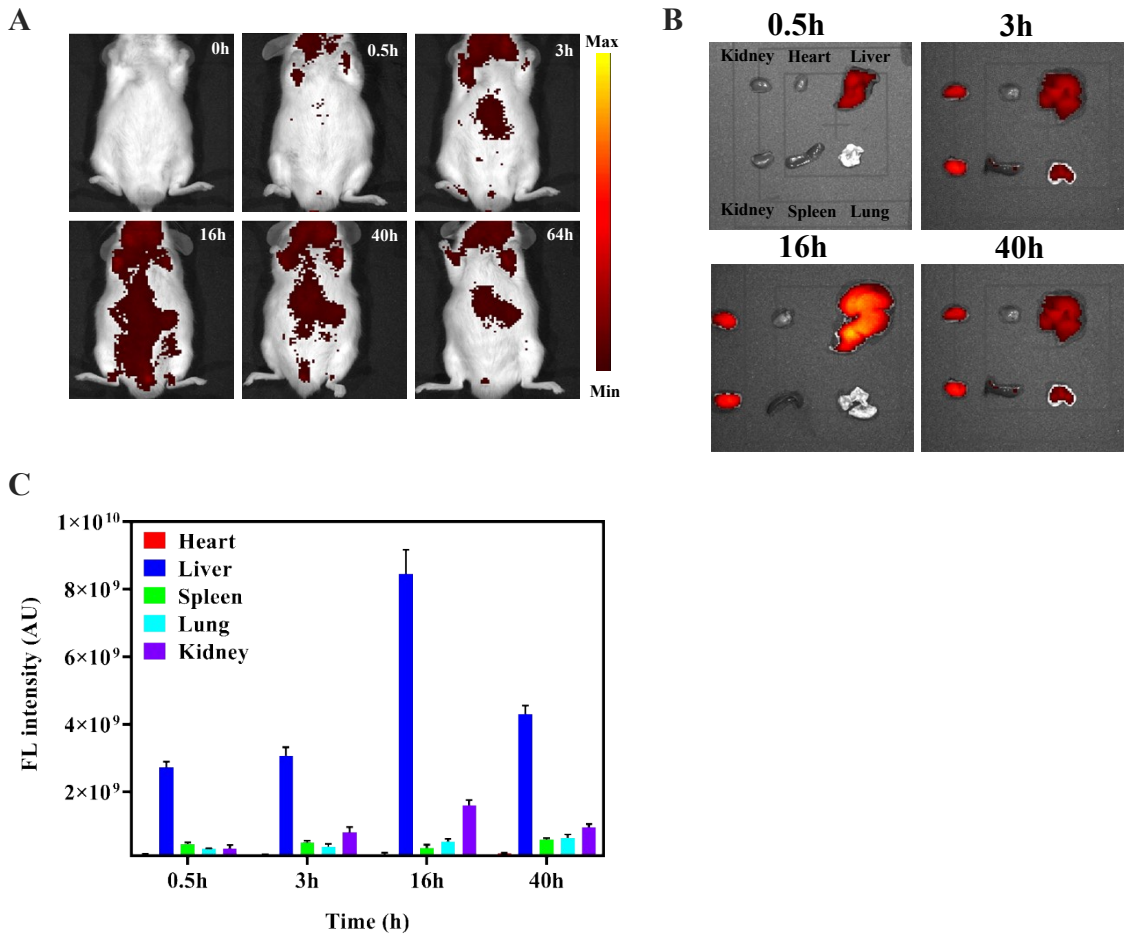

Figure S25. Biodistribution of Cy_{1395}-NPs in healthy mice. (A) Fluorescence images of Cy_{1395}-NPs (2 mg/Kg) at different time (0 h, 0.5 h, 3 h, 16 h, 40 h, 64 h) after injection (λex = 720 nm, λem = 845 nm); (B) Fluorescence images of major organs (Kidney, Heart, Liver, Lung and Spleen) at different times (0.5 h, 3 h, 16 h, 40 h) (λex = 720 nm, λem = 845 nm); (C) Fluorescence intensity of major organs.

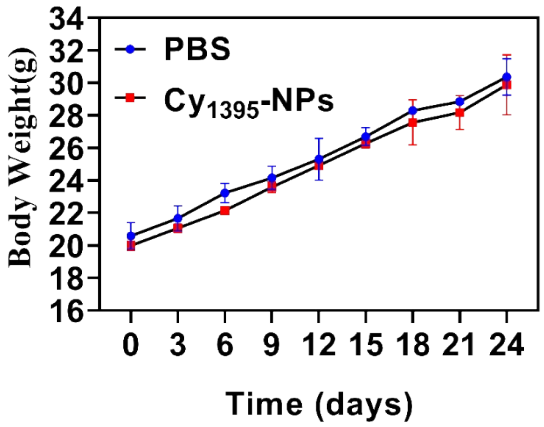

Figure S26. Body weight change of mice within 24 days after injection.

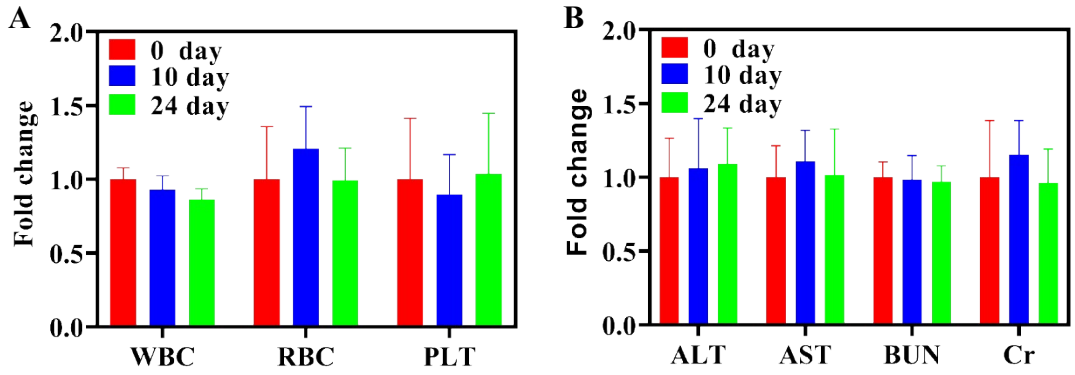

Figure S27. (A) Fold change in white blood cells (WBC), red blood cells (RBC) and platelets (PLT) at different time points after Cy_{1395}-NPs injection (compared with 0 day), (B) Fold change of biochemical (alanine aminotransferase (ALT), aspartate aminotransferase (AST), blood urea nitrogen (BUN) and creatinine (Cr)) at different time points after Cy_{1395}-NPs injection (compared with 0 day).

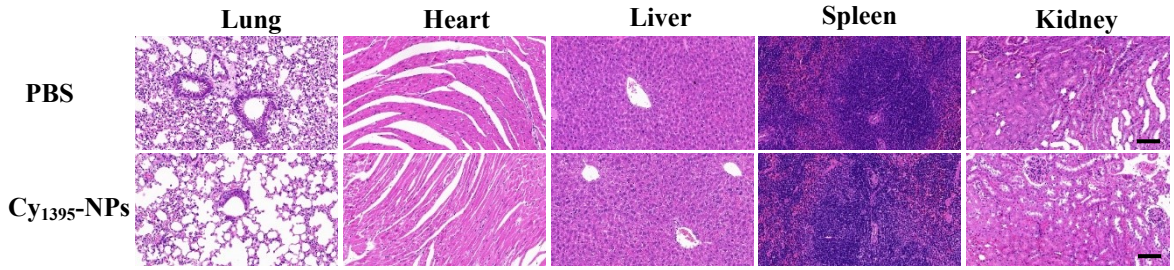

Figure S28. HE sections of major organs of mice in PBS group and Cy_{1395}-NPs group (lung, heart, liver, spleen and kidney; scale bars = 50 μm).

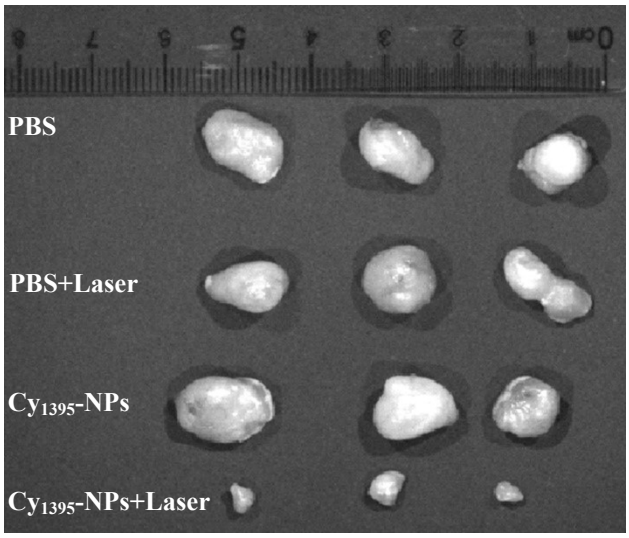

Figure S29. Pictures of tumors in different groups after treatment for 21 days.

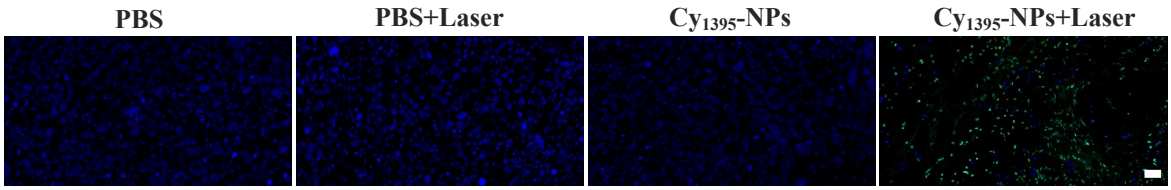

Figure S30. TUNEL fluorescence detect of tumor sections in different treatment groups (Scale bar = 50 μm).

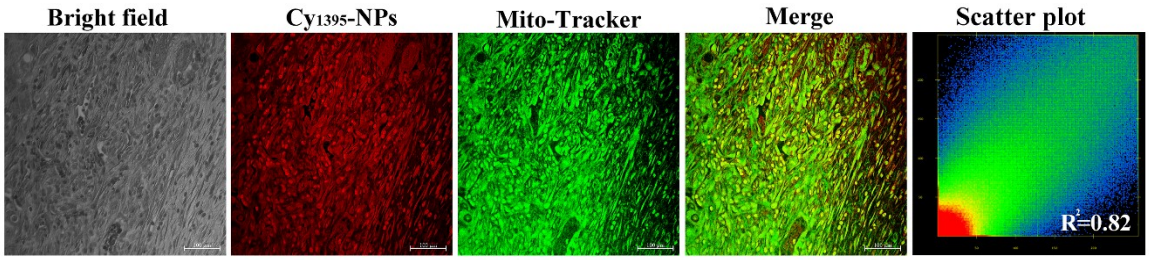

Figure S31. Co-localization fluorescence imaging of Cy1395-NPs in MKN45 tumor section incubated with Cy1395-NPs (10 μM) for 3 h and Mitochondria Tracker for 20 min. The red channel represents Cy1395-NPs, λex=543 nm, λem=600–700 nm; Green channels represent Mitochondria Tracker, λex=488 nm, λem=500–540 nm; scale bars =100 μm. The MKN45 tumor was collected and frozen in Tissue OCT-Freeze Medium, and sliced into 3-μm thin sections. The tumor section was incubated with Cy1395-NPs for 3 hours and Mito-Tracker for 20 minutes respectively, and then washed with cold phosphate buffered saline (PBS). Finally, laser confocal imaging was conducted with 20 objective lens.

References

1. J. Lu, Z. Li, Q. Gao, J. Tan, Z. Sun, L. Chen and J. You, *Analytical chemistry*, 2021, **93**, 3426-3435.

2. E. Kao, M. Shinohara, M. Feng, M. Y. Lau and C. Ji, *Hepatology (Baltimore, Md.)*, 2012, **56**, 594-604.